Curtin

UNIVERSITY OF TECHNOLOGY

Centre for Marine Science and Technology

Model tests on a circular cylinder with appendages

By:
Kim Klaka

REPORT CMST 2001-14

20 August 2001

CENTRE FOR MARINE SCIENCE AND TECHNOLOGY
CURTIN UNIVERSITY OF TECHNOLOGY
PERTH, WESTERN AUSTRALIA

MODEL TESTS ON A CIRCULAR CYLINDER WITH APPENDAGES

The roll motion of a yacht operating at zero Froude number is being investigated. A preliminary step in the investigation is the identification of the factors exerting greatest influence on the motion. A time domain single dof roll simulation (SRM) has been written and a series of full scale trials have been conducted on a sailing yacht at anchor in waves and in calm water. The results indicated that the damping is dominated by appendage viscous and inertia forces. Coincidentally, this is the weakest part of the model in that there is a dearth of experimental data and numerical results for the geometries and environments under investigation. An experimental data set was required for validation of SRM. This was acquired from a set of experiments conducted in a wave basin on a partially restrained model at zero ship speed.

CONTENTS

1 AIMS

The aim of the test program was to generate validation data for numerical models for the prediction of yacht roll motion at zero speed, with particular reference to:

- size of underwater appendage
- cross-section of appendage
- linearity of response with respect to wave amplitude
- effect of wave heading.

2 METHODOLOGY

Two overriding considerations of the methodology were:

- the facilities used were new, the author being the first person to conduct quantitative tests in waves there.
- these were the first set of model tests in this research program, and as such were intended to be exploratory rather than definitive.

The first issue to be addressed was that of scaling. The appendage forces are a function of both Keulegan-Carpenter number (KC) and Reynolds number (Rn)

$$KC = \frac{uT}{D}$$

$$Rn = \frac{uD}{\nu}$$

where

u = velocity - relative velocity in this instance

T = period of oscillation

ν = kinematic viscosity

D = representative length (diameter for cylinders, chord for appendages)

Typical KC values for the appendages range from 0 to 10, with Rn of the order 10^3. Note that it is not possible to compare directly KC numbers for cylinders and flat plates, owing to the use of different reference lengths.

The full hull/appendage system and wave dynamics are subject to Froude number (Fn) scaling dependence.

$$Fn = \frac{u}{\sqrt{gD}}$$

Under Fn scaling the inertial effects and KC will be correctly scaled. Rn will change but the effects are considered negligible for the test geometry and environment under consideration.

The model tests were simplified by using a circular cylinder hull. This hull shape was chosen in order to minimise the wave damping and eddy damping. The canoe body draft was similar in characteristic dimensions to that for the yacht hull used in the full scale trials, in order to retain similar free surface and canoe body influences on the appendages. Three appendage geometries were investigated:

- a full depth rectangular flat plate
- a full depth rectangular aerofoil section keel.
- a half depth rectangular flat plate

The model was free to roll, pitch and heave, with the rig attachment points at the waterline to minimise roll moments caused by sway and yaw restraint. (The transverse metacentre of the circular cylinder model was very close to the waterline.)

There was no requirement for the model to meet any particular scale inertia or transverse stability, provided the values used lay within the bounds of any numerical modelling approximations and assumptions. Attempts were made to keep the roll RAO peak frequency within the range of wave frequencies available in the wave basin. This required the minimisation of roll inertia and maximisation of transverse GM. The variations in keel configuration resulted in small mass and buoyancy changes. Since the objective was to measure the hydrodynamic variations between keels, the mass was allowed to vary whilst keeping the flotation plane and natural roll frequency (in air) constant. The latter was achieved by moving small corrector masses transversely and vertically as required, whilst keeping any changes in roll inertia and transverse metacentric height to a minimum.

Testing was conducted in regular waves rather than irregular waves in the interests of experimental simplicity. The tests were conducted at constant wave amplitude rather than constant wave slope. If constant wave slope were used the amplitudes at the higher frequencies would be too small for accurate measurement. The maximum amplitudes used were determined from constraints of deck edge immersion and rig clearance over the model. Wave steepness was well below the limits for wave breaking.

Free roll decay tests were conducted for two reasons. Firstly, the data would prove useful for comparison with numerical simulation of unforced roll motion. Secondly, they would provide validation data for similar experiments. It is proposed to conduct such experiments at a local facility in the near future. Analysis of the free decay tests was by both the linear and classic (Froude) analysis (Lewis 1989).

3 EQUIPMENT

The model test basin at AMC was 35m long, 12m wide with depth adjustable from 0 to 1m, on a flat floor. The basin was equipped with a multi-element wavemaker, capable of producing normal and oblique regular waves, irregular 2-D long crested and 3-D short

crested waves. The wavemaker was controlled from a dedicated PC using proprietary software. A beach was situated at the downstream end of the basin. The basin sides were vertical.

The instrumentation for these experiments comprised 3 LVDTs and a wave probe. Additional wave probes were used in the preliminary calibration stage. Data acquisition was via signal conditioning and computer logging equipment provided with the facility.

The model was a circular cross section polyethylene stormwater drain pipe, 0.315m diameter and 1m long (*Figure 3-1*). A hollow foam hemisphere was attached at each end to minimise viscous and free surface end effects. The hemispheres were truncated at deck level and were not strictly hemispheric below the waterline - major axis 315mm vertically and transversely and minor axis 300mm longitudinally. A plywood daggerboard case was installed, into which could be slotted one of the three keel configurations. The full and half depth keels were made of 6mm ply, 300m width , and exposed depth 300mm and 150mm respectively. The aerofoil section keel was made by adding a carefully shaped fairing to each face of the full depth flat plate keel. The foil was based on a NACA 0010 section with the aft portion thickened to accommodate a 6mm wide trailing edge. The plywood keels were held in place at deck level by rigid toggles. The model was ballasted with lead ingots held in by Plasticine. The keel-hull join was sealed with Plasticine and/or petroleum jelly. Two plywood platforms were built into the model to accept the rig attachment posts. The model was symmetric both longitudinally and transversely with the following minor exceptions:

- the forward and aft attachment posts were of different mass
- when the aerofoil keel was fitted, the leading edge was placed towards the bow.

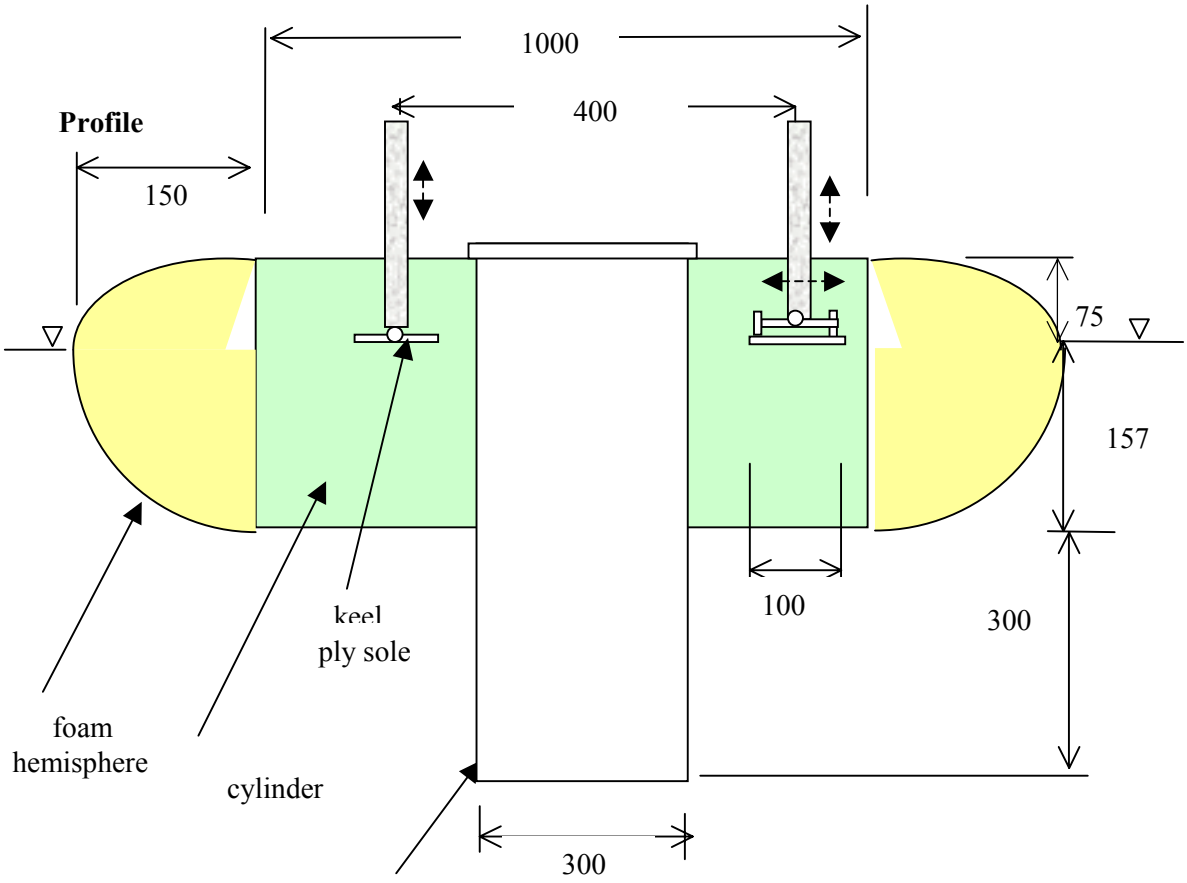

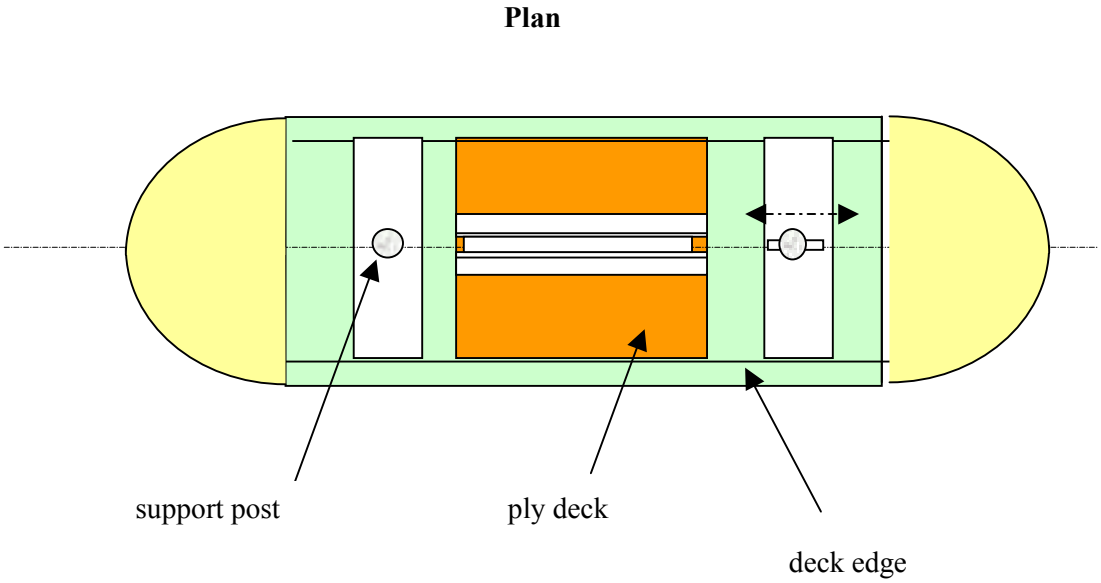

Figure 3-1. model construction

When the keels were changed (always done out of the water), they were re-sealed and the model reballasted to maintain constant flotation waterline, transverse GM and roll inertia. The required ballast modifications were all calculated by spreadsheet, the changes being second or third order effects. The spreadsheet calculated values are shown in *Table 3-1*.

Table 3-1. model variations - calculated by spreadsheet

	full depth keel	half depth keel	aerofoil keel
mass (Kg)	47.12	46.85	48.42
GM_T (m)	0.0991	0.0998	0.0968
BM_T (m)	0.072	0.073	0.070
M below WL (m)	-0.0041	-0.0063	0.0042
VCG below WL (m)	0.0950	0.0935	0.101
Ixx (Kg m2)	0.193	0.193	0.195
nat. roll freq in air (Hz)	2.50	2.50	2.49
moveable ballast (Kg)	1.71	1.71	1.71
transverse location (m)	0.1	0.12	0.0
vertical location below WL (m)	0	-0.02	0.025

The attachment rig for holding the model in the basin consisted of two box-frame support tables, made of approximately 50mm square steel section, each of length 1.5m, width 1m and height 1m. These were placed on the basin floor approximately 3m apart. Two heavy section alloy beams bridged these tables, with the model attachment system and LVDTs connected to the beams. The uprights of the steel tables therefore penetrated the free surface slightly ahead and behind the model, approximately one ship length cross-stream from the model. An earlier rig design which cantilevered the model from a downstream attachment system proved to be too flexible.

The mass of the attachment posts was included in the model mass; their mass moments in roll were not included because they were connected by ball bearings at the waterline (the effective roll pivot point).

4 PROCEDURE

Two wave calibrations were first conducted using an array of 5 wave probes mounted across the basin located 10.8m downstream from the wavemaker . The probes were positioned at 1m spacing, the first probe being 2.5m from the basin side. They were calibrated statically using the basin's in-house software.

The model was weighed and ballasted to the correct waterline based on the spreadsheet calculations, then launched and checked visually against the marked waterline. Next, the model was installed in the first instance across the basin 11.5m downstream of the wavemaker and 5.82m from the working side of the basin i.e. at just under half the basin width, bow away from the working side. The wave probe used during the model experiments was located 0.51m from the side wall and 0.035m downstream of the model (later 0.03m for the oblique wave tests). The LVDTs were calibrated statically. All channels were acquired digitally at 100Hz for 30 seconds without filtering or amplification, and the data stored on floppy disks. This ensured that the (much shorter length of) uncontaminated signal was captured (see 6.3).

The procedure for each run was to program the wavemaker, acquire the zero datum for all recording channels, run the wavemaker, then start acquiring data once the waves reached the model. The wave maker was ramped down on completion of the acquisition and the waves allowed to die down before the next run - generally about 20 minutes later. The instruments were recalibrated at the beginning of each day and when a measurement problem was suspected.

On completion of the beam sea tests, the support tables and attachment system were moved so as to align the model 120 degrees to the waves (following seas defined as 0 degrees). A number of runs were also conducted in calm water to measure the free roll decay and to carry out an inclining experiment. Heel angles in the latter were measured using the LVDTs. Water temperature and water depth were recorded at intervals throughout the experiments.

Photos and video footage were taken at various times during the tests.

At the end of the tests the model was re-weighed then mounted on a roll table, and the vertical centre of gravity and roll inertia were measured. The roll table comprised a frame on which the model sat, pivoting about a longitudinal axis. A mass could be moved along a rod perpendicular to the axis for trimming purposes. The mass was first shifted to a point such that the VCG of the frame (without model) was at the axis, as determined by balancing. The model was then placed on the frame, care being taken to align it in heel, sway and yaw. The vertical (heave) position of the model was then adjusted until the total VCG was again at the axis. The distance from the waterline to the axis was recorded as the VCG of the model.

The roll inertia of the model was found by assuming the system to be an undamped single degree of freedom system. The trimming mass was moved through a measured distance and the period of oscillation measured for the model plus frame. The model was then removed and the period measured for the frame only. The roll inertia of the model was found from

$$I_{xx} = \frac{gmd(T_2^2 - T_1^2)}{4\pi^2}$$

where
I_{xx} = roll moment inertia
g = acceleration due to gravity
m = trim mass
d = distance trim mass is moved

T_2 = period of table+model
T_1 = period of table

The pitch inertia was not measured.

5 ERRORS

5.1 Model and keels

The three main sources of error in the model were:

hull twist

During construction it was not possible to constrain entirely the torsion inherent in the polyethylene pipe. This became evident when ballasting the model to its flotation waterline. There was a transverse discrepancy of 1.5mm between the water levels forward and aft, representing a twist of 0.3° over the length of the model. Whilst this did not impact significantly on the geometry, the hull being circular section and the keel being upright relative to the mean twist angle, the longitudinal distribution of ballast was difficult to replicate accurately. The effect of this on the results is not readily quantified.

keel warp

During construction a chordwise camber of up to 1% developed in the keels, though this effect diminished on immersion in water. A method of estimating the error induced has not yet been identified.

water absorption

The main hull of the model did not leak but there was an air gap of up to 2mm between the hull ends and the hemispherical end pieces. There was also an 8mm diameter hole inside the end pieces along the longitudinal axis on the waterline. Whilst these were sealed with filler and plasticine, the quantity of water dripping from the model when removed from the water implied that the seal was not 100% effective. The main error this would have created was on the transverse second moment of the waterplane, with a reduction of up to 0.4%

Water absorption of the model itself can be estimated from change in model mass throughout the experiments. The mass of the model with full keel was 46.92Kg at the start of experiments and 47.07Kg at the end. The discrepancy of 0.3% is probably due to water absorption. The scales used showed readings repeatable to +-0.005Kg.

5.2 Vertical centre of gravity and roll inertia

The VCG determined from the roll table experiment was 2.7% higher than the figure obtained from the inclining experiment. The VCG calculated by spreadsheet was a further 2.6% higher. Variations in spreadsheet calculation of BM of up to 3% were evident, depending on integration approximations made. Variations in the mass moment of inertia calculation were considerable. The inclining experiment analysis required hydrostatic data from the spreadsheet (see 6.1.1), so those estimates were not independent. The heel angles measured during the inclining experiment were repeatable to within 0.2° (0.75%), with 95%

confidence limits of 0.1° in the time series. The applied moment was accurate to within 1%. The errors in the roll table measurement were mainly due to alignment of the model and friction in the bearings. No estimate of these errors was made.

The measured roll inertia was 0.0604 $Kgm^{2.}$. The timed periods were repeatable to within 3% (*Table 6-2*), the mass measured to within 0.3% and the distance moved 10%. When these errors were propagated through the calculation, the estimated error in the inertia was 25.5%. . The spreadsheet estimate of inertia was 0.193 Kgm^2 . This is a 300% difference, probably due to an error on the roll table experiment (see 6.1).

5.3 Wave measurement

5.3.1 Calibration

The data acquisition system did not record the raw calibration data, but displayed it on the screen. The figures for two calibration sets were written down from the screen display and processed in a spreadsheet. The 95% confidence limits of the calibration data were +-0.31mm for the wave probe used throughout the tests. This amounts to 2.2% error for the median wave standard deviation used.

5.3.2 Spatial variation

Figure 6-2 shows the spatial differences at a high frequency. The variations are +-3% about the mean value. Up to half of this may be attributable to the calibration error described above. The variation at other frequencies and amplitudes is not known.

The phase angles of the wave probes were found to differ between each other by less than +-3°.

5.3.3 Time variation

The time variation was assessed by calculating the standard deviation of the surface elevation for 6 different data segments within a typical run. At 0.5 Hz (run 10) they varied by +- 2.7%. At 0.8 Hz (run 7) they varied by +-1%. The amplitude varied by 14% and 4% respectively.

5.3.4 Other issues

The uprights of the attachment rig tables protruded through the free surface, resulting in wave diffraction. However, the diameter/wavelength ratio was always less than 0.03 so the effects were small.

Run-up on the wave probes would introduce errors, particularly in phase measurements. However, the presence of this error source was not investigated.

5.4 motions measurement

The 95% confidence limits of the static calibration data were +-0.4mm and +- 0.48mm for the port and starboard LVDTs respectively i.e +-0.2° roll. This amounts to 3.5% error for the mean roll standard deviation. The error induced by time variation was assessed by calculating responses for 6 different data segments within a typical run. At 0.5 Hz (run 10) the roll RAO varied by +-2.3% over the segments. At 0.8 Hz (run 7) the roll RAO varied by +-1.7% .

It was noted that the LVDT signal contained a 12Hz and 43 Hz noise, with standard deviation varying from unmeasurably small at mid range to 0.14mm at 70% full scale deflection. *Figure 5-1* shows the signal from the starboard LVDT when it is disconnected from the model and fixed at 70% full scale deflection. The zero datum for the LVDTs was often near 50% fsd. This resulted in up to 3% error (95% confidence limits) in the roll motion, depending on the motion frequency and amplitude.

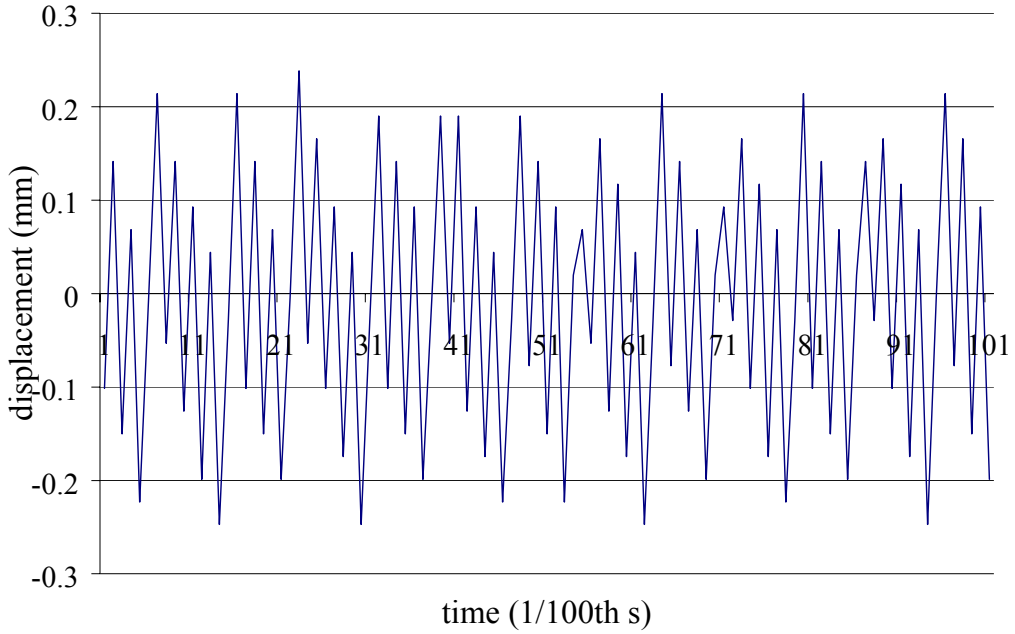

Figure 5-1. stbd LVDT noise - zero datum is at 70% f.s.d.

It was observed that the LVDT strings went slack at the upper limit of travel on run 34 due to friction in the barrel. This problem was rectified and the run conditions repeated. The difference in roll RAO was 4%. This phenomenon was not noticed in other runs. The overall error (95% confidence limits) for the roll and heave motion RAOs is estimated as +-7%. The percentage errors in pitch motion are an order of magnitude greater, owing to the small absolute values of motion.

The error in measuring the downstream separation distance of the model and the wave probe was +-5mm This translates to a phase error ranging from 1.2° at 1 Hz to 0.3° at 0.5Hz. Larger phase errors are likely to have resulted from the noise in the LVDT signals. Wave probe run-up would also have contributed to phase errors. The programmed wave frequencies were correct to +-0.5%. If this were considered a direct phasing error it would amount to +-18°. The frequency distribution of the phase angles near the motion spectral peak implied that errors of this magnitude were present.

For waves which are nonlinear, the linear dispersion relationship

$$\omega^2 = gk(\tanh(kd))$$

should include a nonlinear correction of $1 + ka^2$ (O'Dea, Powers & Zselecsky 1992)

where

ω = wave radial frequency

k = wave number

d = water depth

a = amplitude of wave first harmonic

This corresponds to a maximum error of 1.5% (5°), for the tests conducted at 0.03m wave amplitude. This reduces to less than 0.6% (2°) for the wave amplitude of 0.02m used for the majority of the tests.

Overall phase errors are estimated at 20° (5%).

5.5 other factors

Water temperature of 15°C varied by 1°C over the period of the tests.

The location of the model in the tank was measured to within +-0.1m. This translates to a wave heading error of +- 0.5°.

The water depth was measured several times during the experiment at various positions in the tank. The maximum variations were +-3mm (0.4%).

6 RESULTS AND DISCUSSION

6.1 Centre of gravity and roll inertia

The vertical centre of gravity was estimated by two independent methods - inclining experiment and roll table.

6.1.1 Inclining experiment

The inclining experiment was conducted with the full depth keel attached. The mean heel angles were as shown in *Table 6-1* below.

Table 6-1. inclining experiment results

run number	42	43	44
mass moved (Kg)	0.82	0.82	0.82
transverse shift (m)	0.0	0.25	0.0
heel angle (°)	6.740	4.079	6.742
95% confidence limits (°)	0.11	0.08	0.09

The resulting mean heel angle of 2.66° yielded a transverse GM of 0.094m. Using the spreadsheet-calculated BM value in *Table 3-1*, the VCG was 0.090m below the waterline. The spreadsheet-calculated value of VCG was 0.095m below the waterline.

6.1.2 Roll table experiment

The VCG of the model with half depth keel was found to be 0.0925m below the waterline from the roll table experiment. This compares with the spreadsheet calculated value of 0.0935m. The inertia oscillation results for the model are shown in *Table 6-2*, with a trim mass of 1.866Kg moved through 0.10m. Note that this was for the model without the attachment posts. The roll inertia of the attachment posts was negligible because they were hinged at the waterline (effectively the roll centre).

Table 6-2. roll table oscillation periods

time (s) model + table; for 5 oscillations	time (s) table only; for 10 oscillations
12.7	22.72
12.85	22.74
12.78	23.03
mean period = 2.553	mean period = 2.283

The results yielded a roll inertia estimate of 0.0604 Kgm^2 using the method described in section 4. The spreadsheet estimate of inertia was 0.193 Kgm^2. This is a 300% difference. A subsequent bifilar suspension experiment was conducted for the unballasted model, the results of which agreed with the spreadsheet estimate within 6%. It is concluded that an error was made in the roll table experiment

6.2 Free roll decay

Roll decay tests were conducted for two runs with full depth keel. The time series are shown in *Figure 6-1*. Whilst the natural periods agree closely, the damping differs between the two runs. Neither the Froude nor the linear analysis yielded consistent results, the values determined being highly sensitive to the segment of the data set used. Mean values and range are given in *Table 6-3*. The differences are quite possibly due to non-linearities introduced through the different initial heel angles for each run.

Table 6-3. roll decay results

	mean period (s)	β	k1	k2
run 17 - mean	1.70	0.309	1.04	-2.44
run 18 - mean	1.57	0.183	0.684	-1.78
error range +-	0.2	0.15	0.7	0.7

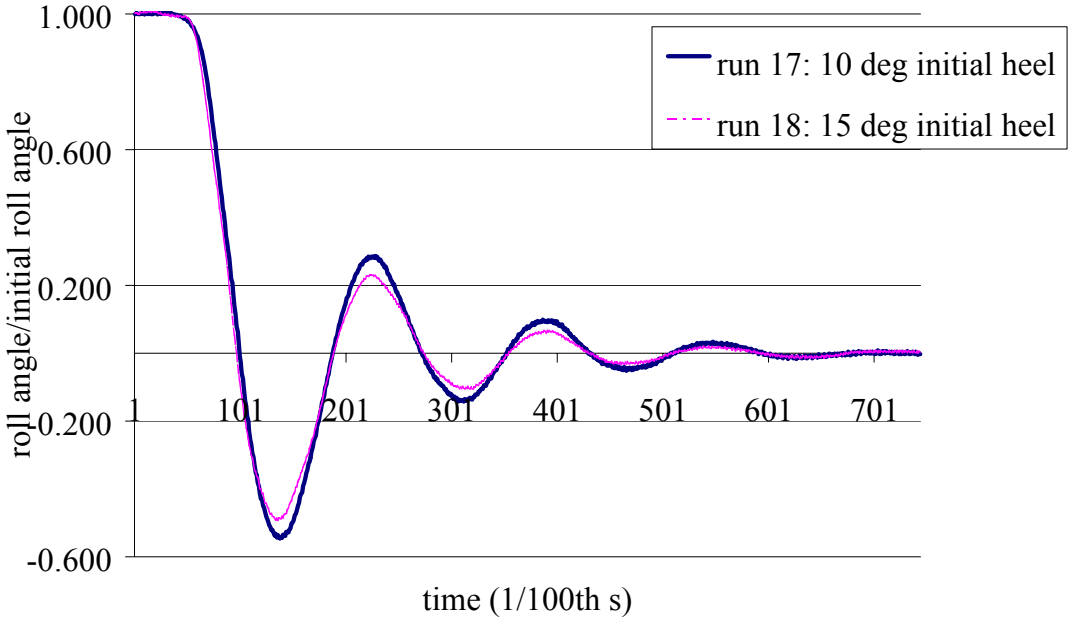

Figure 6-1. roll decay time series

6.3 Wave field variation

Before the model and attachment rig were installed, two consecutive runs were taken with the 5 wave probe array in waves of frequency 1Hz and nominal amplitude 0.02m. On the second run an additional probe was mounted near the basin sidewall. This was the probe from which wave measurements were taken when the model was in place. The spatial variation of the surface elevation standard deviations across the basin is shown in *Figure 6-2*.

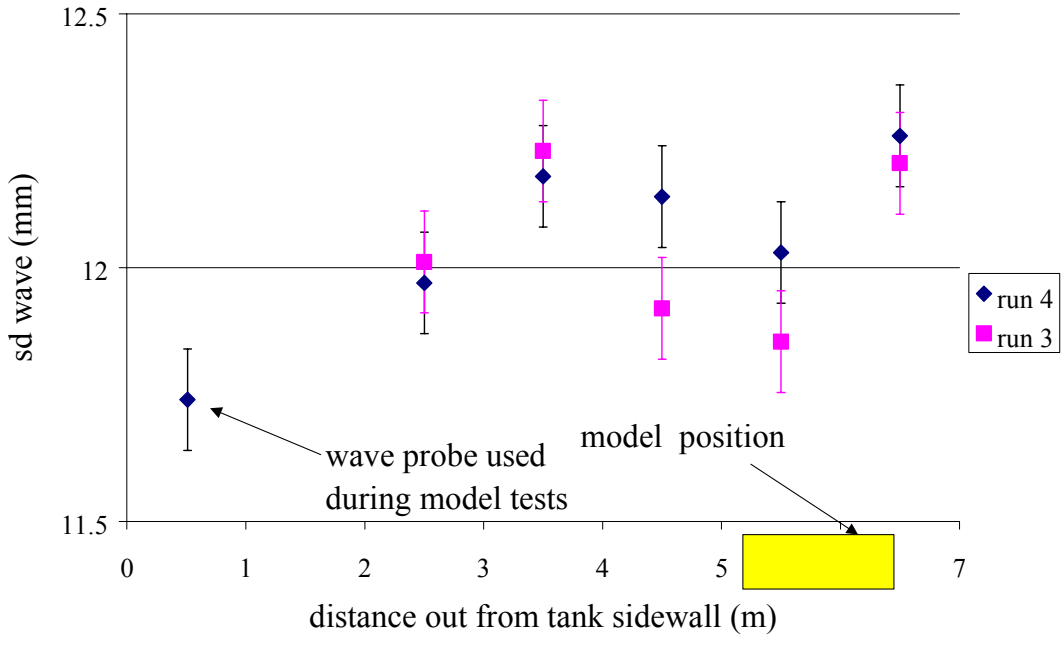

Figure 6-2. spatial variation of waves

The error bars represent the range of standard deviations of data taken from 7 different samples of the time series. The spatial variations impacted on the results in two ways:

- The attenuation of the wave amplitude at the probe used for the model experiments is not well described. This introduces uncertainty in the repeatability of the tests at a later date, particularly if a different facility were used.

- The wave amplitude varied significantly over the length of the model.

The temporal variation of the waves was a function of frequency, as evident from *Figure 6-3* and *Figure 6-4*.The wave ramp up period is evident in approximately the first 5 seconds of data in *Figure 6-3* and the influence of reflected waves can be seen from approximately 12 seconds into the data of *Figure 6-4*. It became evident from these data sets that 0.5 Hz was the lowest practicable frequency if the time variations were to be kept within acceptable limits and the data set was to contain a sufficient number of cycles before reflected waves arrived at the probe. Even within these constraints, the amplitude varied by 4% at a wave frequency of 0.8 Hz and as much as 14% at a wave frequency of 0.5 Hz. The standard deviations varied by 1% and 2.7% respectively. The temporal variation of wave elevation had significant impact on the motions data processing techniques, as described in section 6.4.

The ramp up process of the wavemaker may have contained low frequency components. When these low frequencies were reflected off the beach and back to the wavemaker, they resulted in low frequency variation of the water depth at the wavemaker. This could have caused amplitude modulation if the stroke amplitude of the wavemaker required to generate a particular wave amplitude was a function of water depth at the wavemaker.

A frequent cause of temporal variation is the presence of standing waves. However, this does not result in amplitude modulation, rather it introduces a low frequency component. For completeness, the seiching frequencies of the basin were calculated as follows:

For shallow water waves the natural seiching period of a closed basin is

$$T = \frac{n\sqrt{gd}}{2L}$$ (Pond & Pickard 1983)

where

T = period

n = integer 1,2,3...

d = basin depth

L = basin length

The effective length of the basin from the wavemaker face to the end wall was 30m, yielding natural periods of 23s, 11.5s etc. The presence of the beach may have reduced these periods slightly.

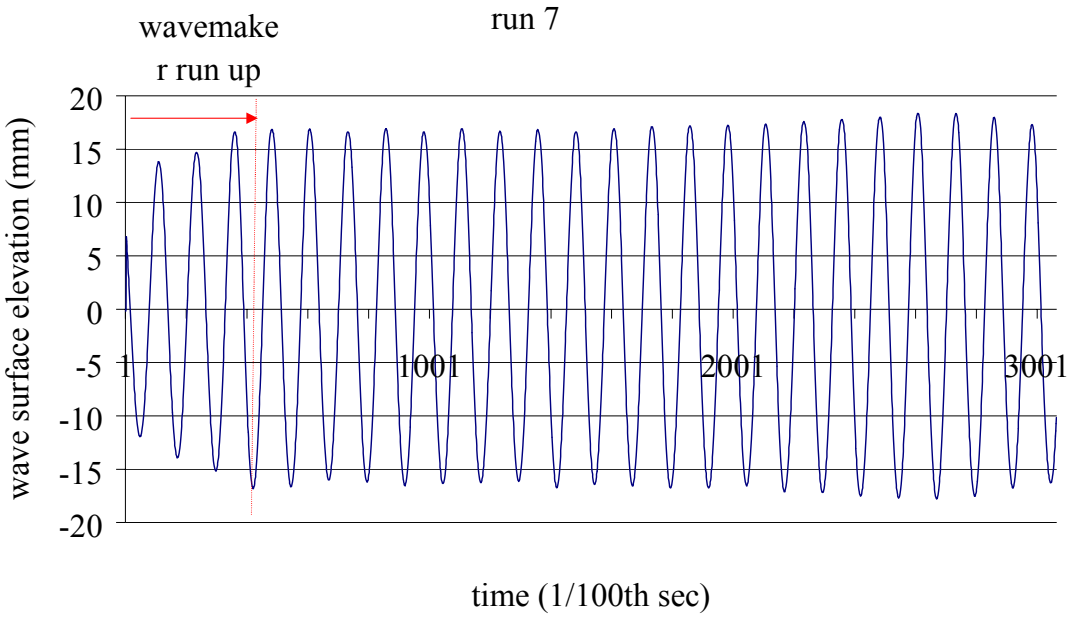

Figure 6-3. time variation of waves - 0.8 Hz

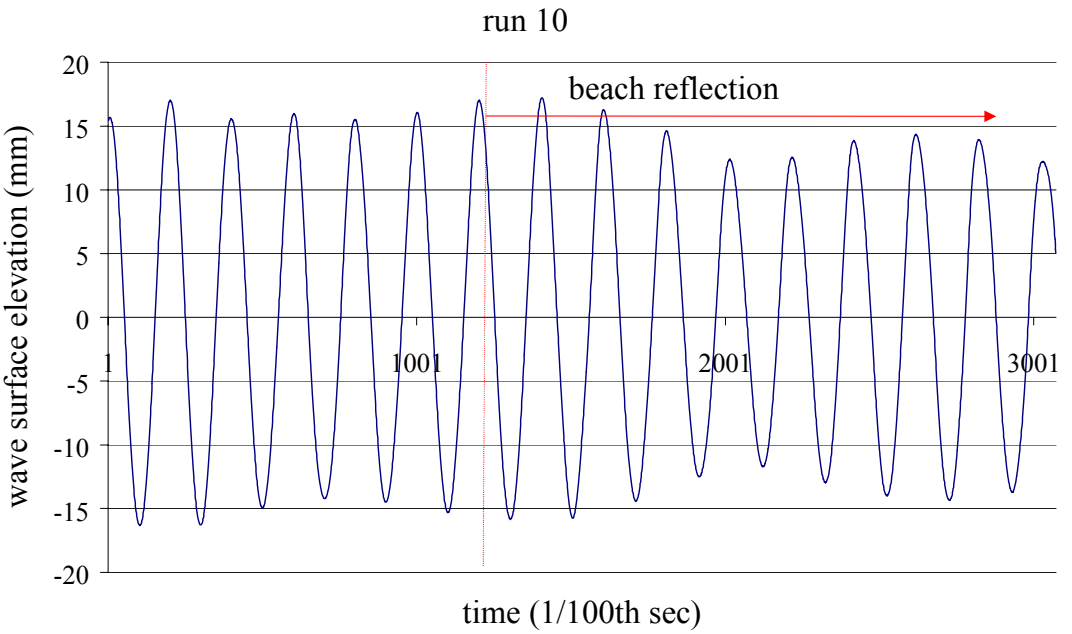

Figure 6-4. time variation of waves - 0.5 Hz

6.4 Motions data processing

It was evident from the variation of the wave field that the motions data required particularly careful processing if errors were to be kept within acceptable bounds. The frequency programmed into the wavemaker software was found to be correct to within +- 0.5%, so the main issue was surface elevation. Spatial variation was accounted for by calculating a

correction factor from the standard deviations, to determine the wave surface elevation at the model from the measurements taken at the side probe. This did not necessarily take into account the influence of the attachment rig on the wave field, nor did it allow for the possibility of the attenuation factor varying with wave frequency or amplitude.

Temporal variation of the waves was dealt with more thoroughly. Firstly, the captured data set had to extend from the end of the wave ramp-up period to the arrival of the refleced waves. The sample length was set at 30 seconds to achieve this. The raw data were calibrated then mean subtracted. The attenuation factor was applied to the wave probe signal and it was then phase shifted to account for the downstream separation between the probe and the model, using full intermediate depth linear wave theory. The required data segment was then chosen interactively from graphical inspection of both the wave and roll motion data, in an attempt to exclude the ramp up and reflection effects. The selected data set was then reduced to the nearest number of integer cycles and the standard deviation was calculated. Standard deviations were then used throughout any subsequent processing. Amplitudes were calculated (for display purposes only) from the standard deviation by assuming the signal was sinusoidal.

The motion phases were calculated from the complex transfer function. This was checked firstly against the argument at the peak value of the real part of the ratio of Fourier transformed output and input signals, secondly against the positions of the signal peaks in the time series.

6.5 Linearity of roll with respect to wave amplitude

Tests were conducted with the full depth keel in beam seas for three nominal wave amplitudes over a range of frequencies. The results are shown in *Figure 6-5* and *Figure 6-6*, .

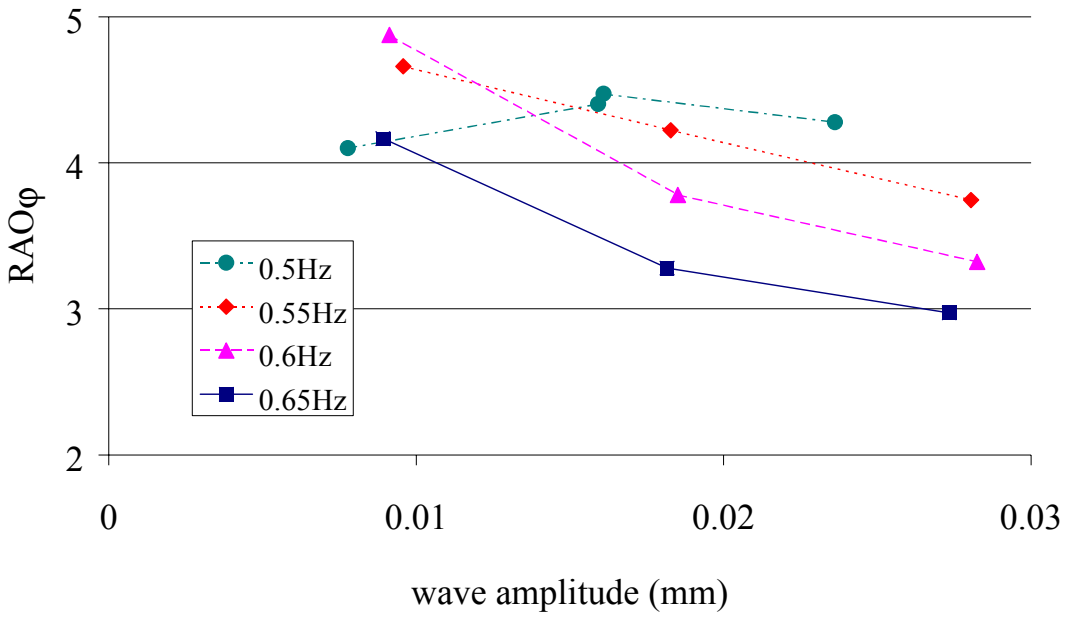

Figure 6-5. effect of wave amplitude on roll response

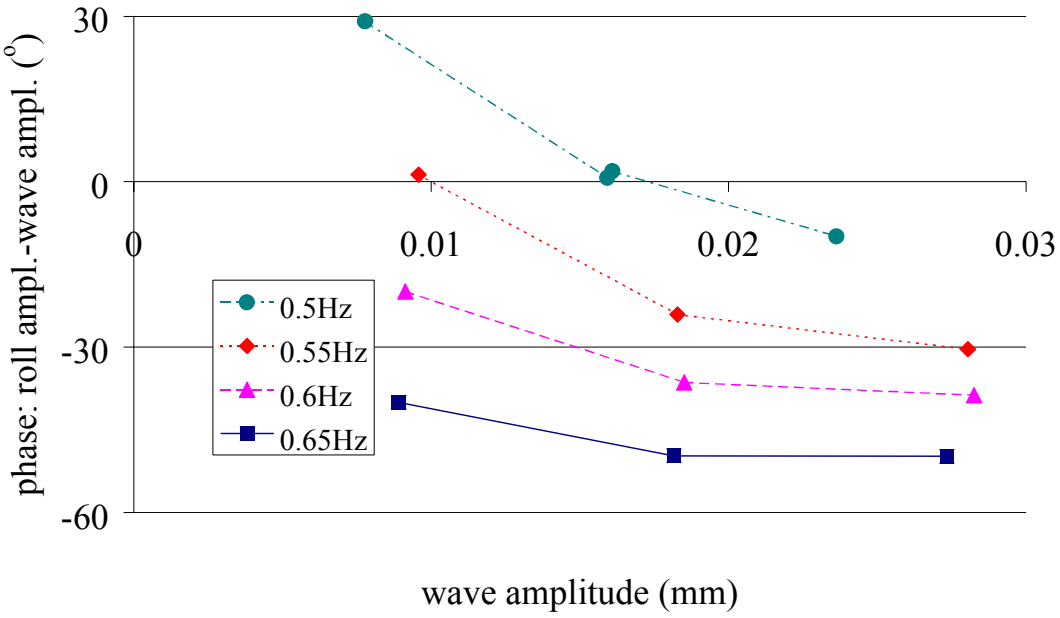

Figure 6-6. effect of wave amplitude on roll phase

The results are not unexpected, as roll motion of appended vessels is usually non-linear (Robinson & Stoddart 1987), (Spouge 1991).

6.6 Effect of appendages on roll

The influence of appendage configuration is shown in figures *Figure 6-7* and *Figure 6-8*. The latter is the same data presented in non-dimensional form, using

$$w = \omega\sqrt{\frac{B}{g}}$$

and

$$RAO\varphi = \frac{\varphi_s}{k\zeta_s}$$

where:
ω = wave radial frequency
B = waterline beam
g = acceleration due to gravity
ζ_s = surface elevation standard deviation
φ_s = roll angle standard deviation
k = wave number

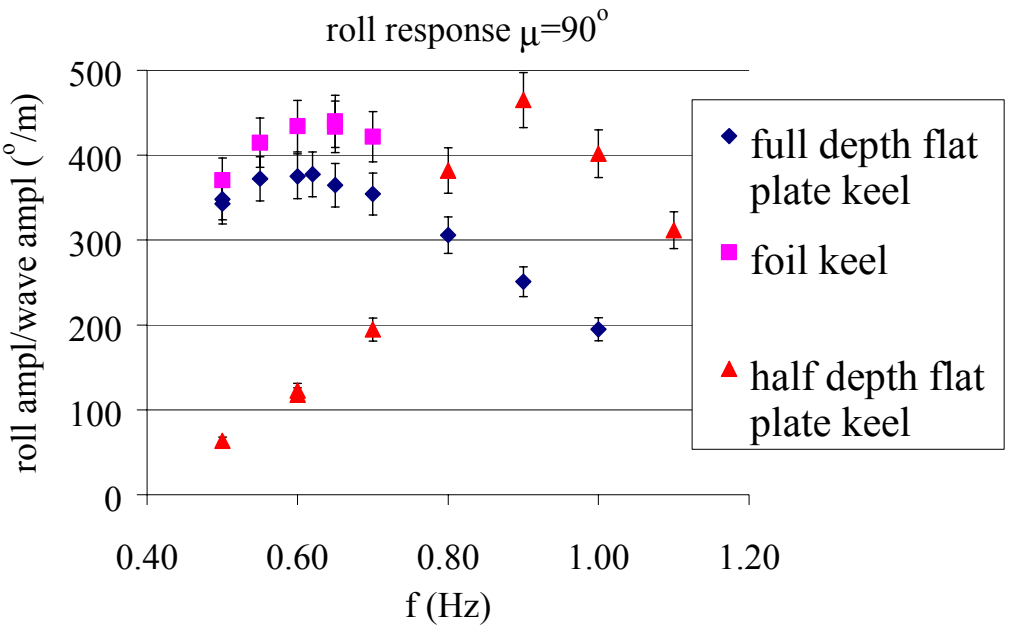

Figure 6-7. effect of appendages on roll amplitude

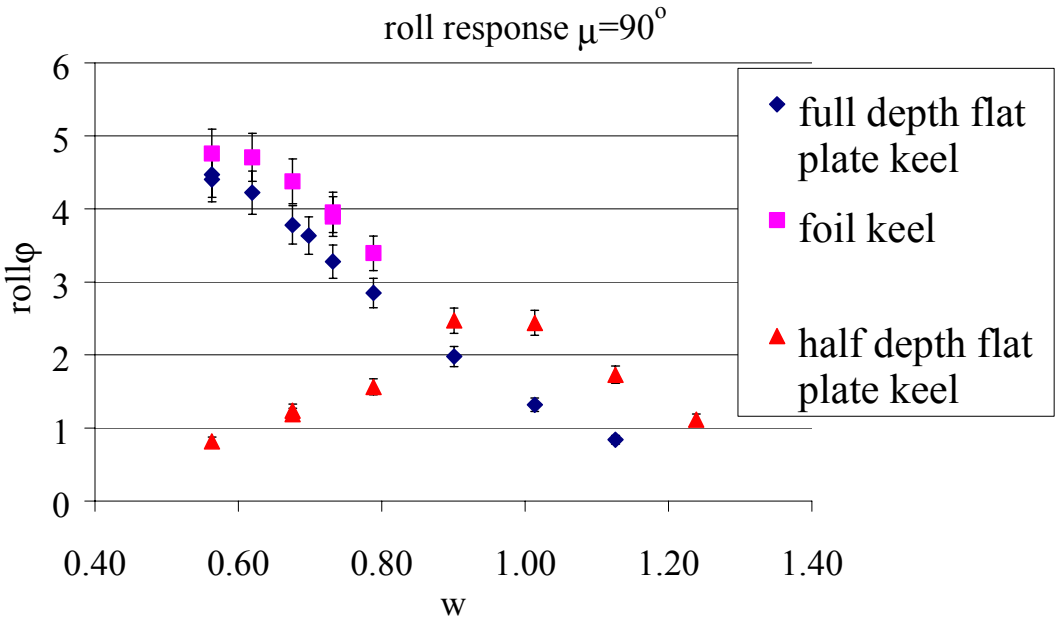

Figure 6-8. effect of appendages on roll amplitude - non-dimensional display

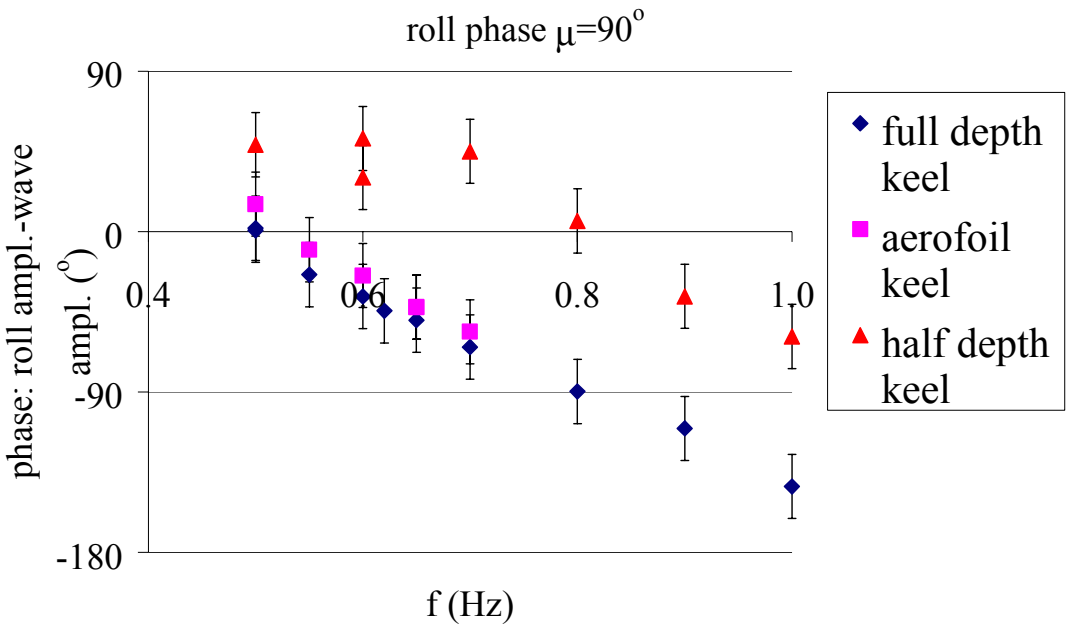

Figure 6-9. effect of appendages on roll phase

6.6.1 Frequency of peak response

The non-dimensional presentation of the results shows that the frequency of peak response for the full depth and aerofoil keels was at or possibly below the lowest frequency used in these tests. The peak frequency from a range of sources is shown in *Table 6-4*.

Table 6-4. comparison of peak frequencies (Hz)

source: (Hz)	full depth keel	aerofoil keel	half depth keel
RAO	0.5	0.5	0.85
amplitude	0.62	0.62	0.9
phase	0.5	0.52	0.8
free decay	0.59 - 0.64		

The RAO value is from the dimensionless plot (*Figure 6-8*), the amplitude value is from the dimensional plot (*Figure 6-7*). The phase angle at resonance for a lightly damped single dof system is 90° between input and output. For a rolling vessel , this corresponds to the phase between the wave slope and the roll angle. *Figure 6-9* shows phase between roll motion and wave amplitude, which is 90° lagged from wave slope. Therefore resonance occurs at a phase of 180° in this plot .

For the full depth keel, the frequency of peak response from the RAO and phase sources agree well. This contrasts with the natural frequency in the free decay tests. The peak amplitude occurs at the resonant frequency of the free decay tests. The values for the aerofoil follow those of the full depth keel. The values from the various sources for the half-depth keel are in closer agreement with one another.

Two observations are made:

The difference in peak frequency between the half depth and full depth keels is considerable, and is most likely attributable to a very large added inertia change. This might also be linked to a sea bed effect, though the keel clearance is large (>30% of water depth).

The discrepancies between the frequency of peak response in waves and that found in the free decay tests is not so readily explained. The forcing function varies with frequency, so the resonant frequency is not necessarily the frequency of peak response. The resonant frequency is often amplitude dependent for non linear motions, and the roll amplitudes in the free decay tests were lower than for the wave tests near resonance. However, the tests conducted at different wave amplitudes do not reveal any significant shift in resonant frequency (*Figure 6-5*).

6.6.2 Damping

The damping of the aerofoil keel is typically 12% greater than for the (flat plate) full depth keel. This may be a result of changes in vortex generation round the aerofoil keel due to the rounded edges, particularly the leading edge. The non dimensional plot of *Figure 6-8* shows that the dimensionless response amplitude of the half depth keel is approximately twice that of the full depth keel. This is counter-intuitive and is quite probably a consequence of the different peak frequencies. The wave force at a particular frequency will most likely be different for the two keels, owing to the difference in lateral area and draft. This makes comparison difficult. The dimensional plot of *Figure 6-7* shows the peak roll response for the half depth keel to be approximately 20% higher than for the full depth keel, albeit at a different wave frequency. This result may be explained by some combination of :

- the reduction of edge length, hence reduction in vortex-induced damping, for the half depth keel compared with the full depth keel;
- the change in wave force due to the reduced keel draft.

If the results are placed in the context of a full scale yacht rolling at anchor, then for a constant wave amplitude spectrum the full depth keel will roll less than the half depth keel, whereas for a constant wave slope spectrum the opposite is true.

6.7 Effect of wave heading on roll

Both the full depth keel and the half depth keel were tested at wave headings of 90° and 120°, at nominal wave amplitude 0.02m. The results are shown in *Figure 6-10* to *Figure 6-13*. These are in broad agreement with the output from the Simple Roll Model and with experiments on other hull forms (Bhattacharyya 1978), and contrasts with the findings from the full scale trials (Klaka 2000). This supports the hypothesis that the directional spread of waves in the full scale trials disguises any effect of wave heading, though the effect of yaw restraint might also be a factor.

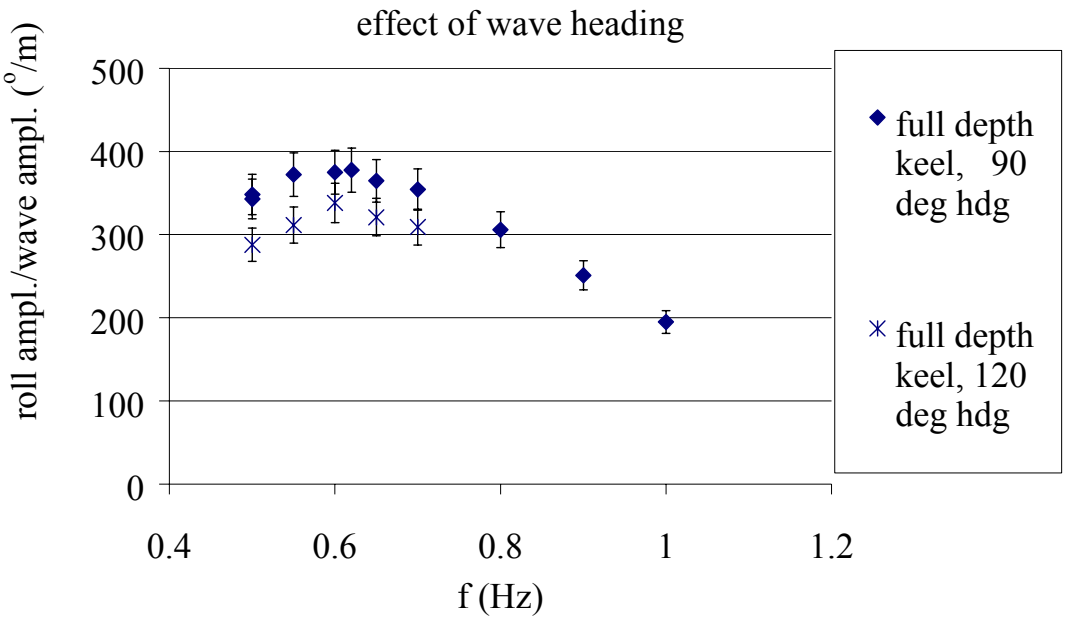

Figure 6-10. effect of wave heading on roll amplitude - full depth keel

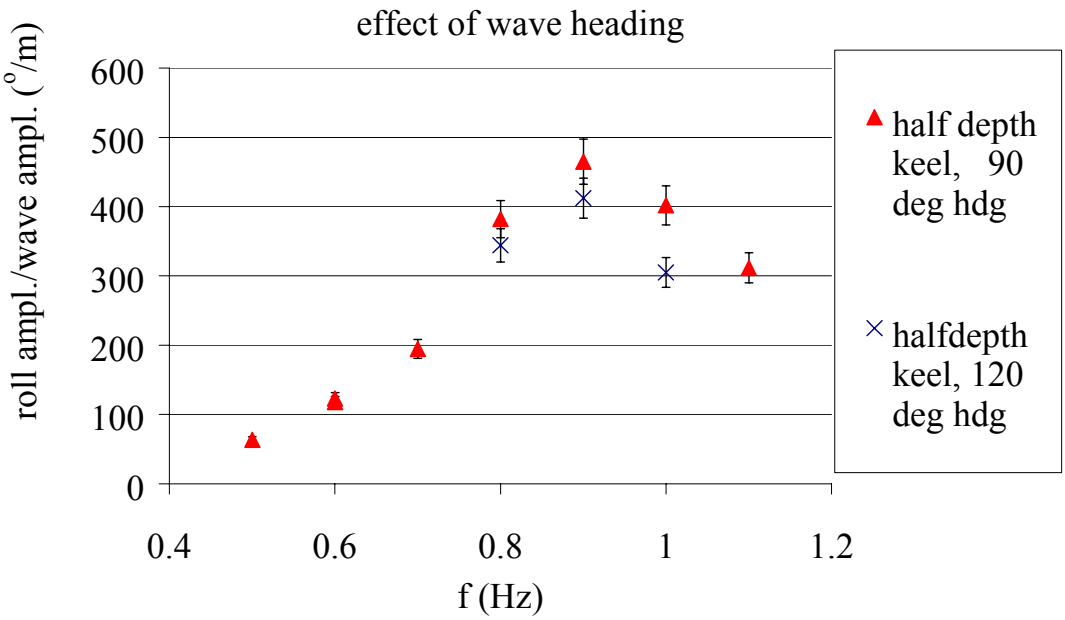

Figure 6-11. Effect of wave heading on roll amplitude - half depth keel

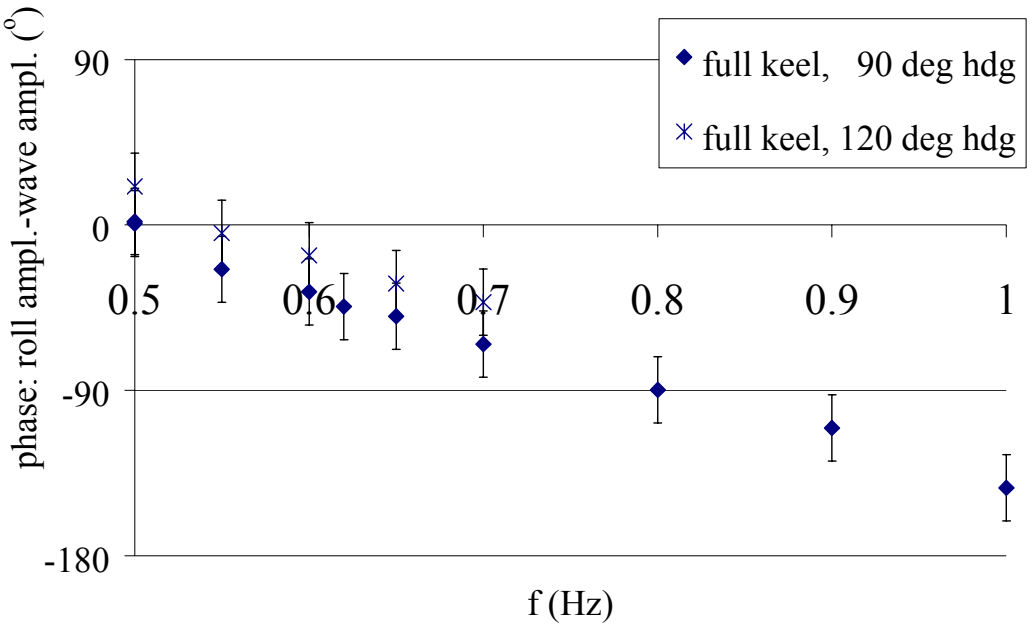

Figure 6-12. effect of wave heading on roll phase - full depth keel

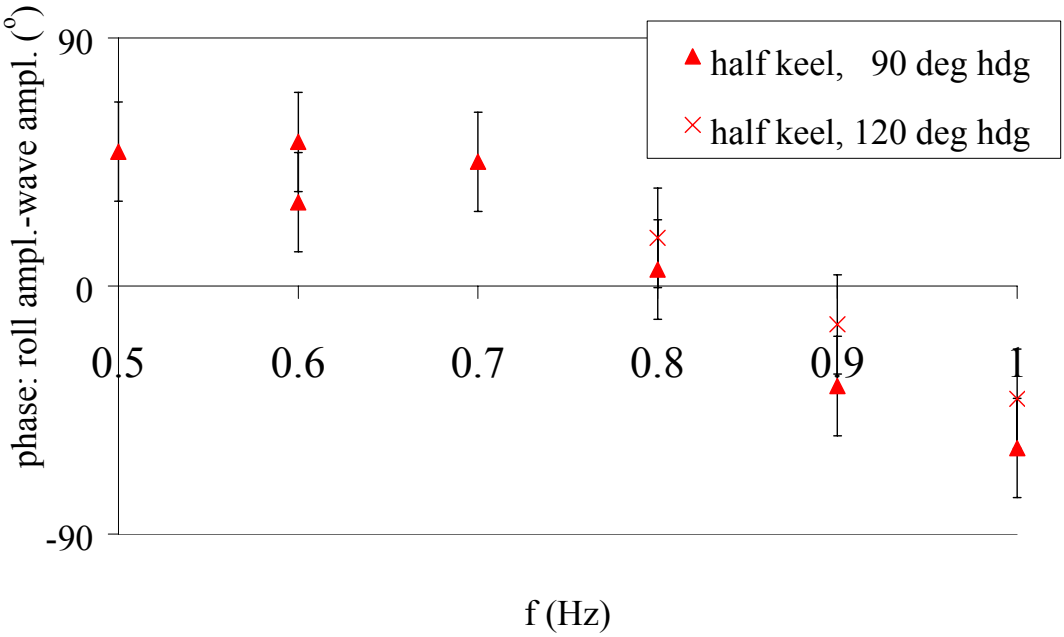

Figure 6-13. effect of wave heading on roll phase - half depth keel

6.8 Heave and pitch motions

The heave and pitch RAOs for the full keel are shown in *Figure 6-14* and *Figure 6-15* at both 90° and 120° heading. The corresponding phase angles are shown in *Figure 6-16* and *Figure 6-17*. The pitch data at 90° in particular are subject to very large percentage errors

due to the very small motion amplitudes. The results for the other keel configurations are similar. All the results are well behaved in so much as the heave RAO is close to unity at low frequencies while the pitch RAO is negligible in beam seas, increasing in oblique seas. The heave resonant frequency is at some value greater than 1Hz.

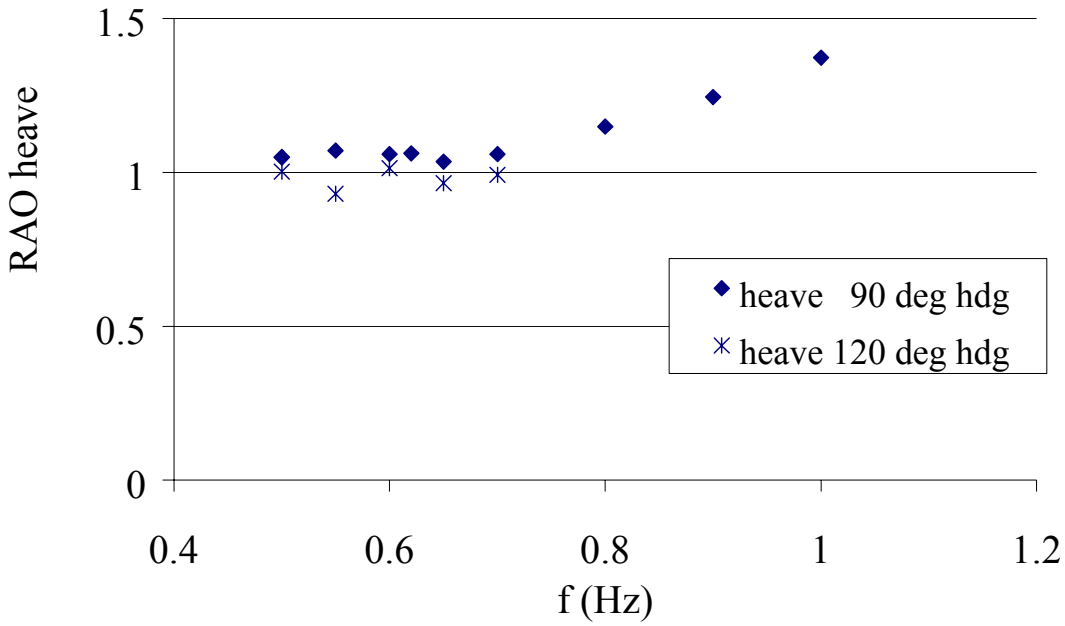

Figure 6-14. heave RAO - full keel

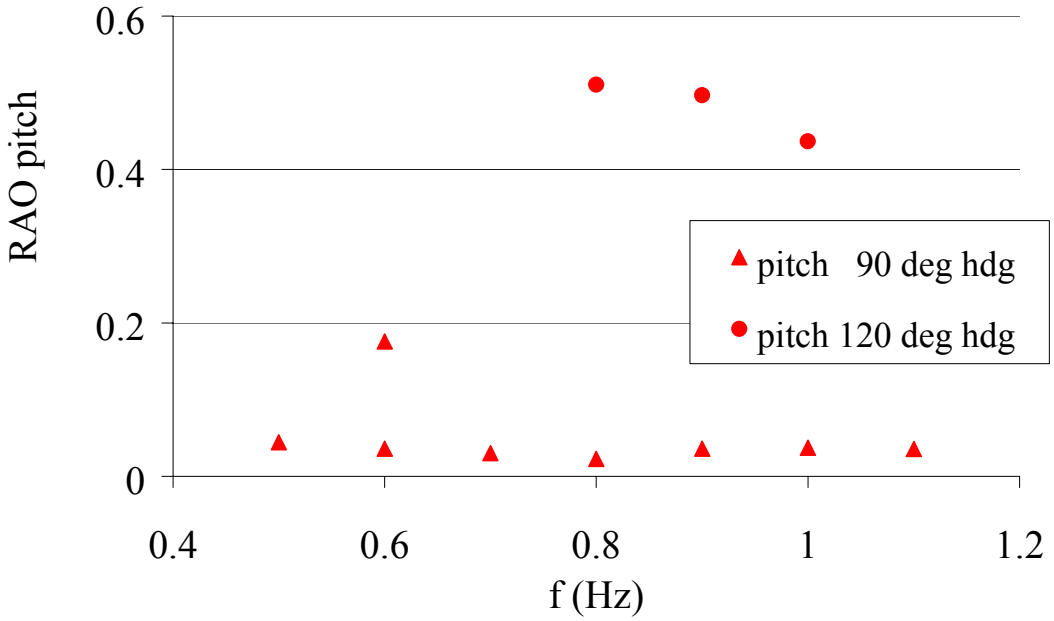

Figure 6-15. pitch RAO - full keel

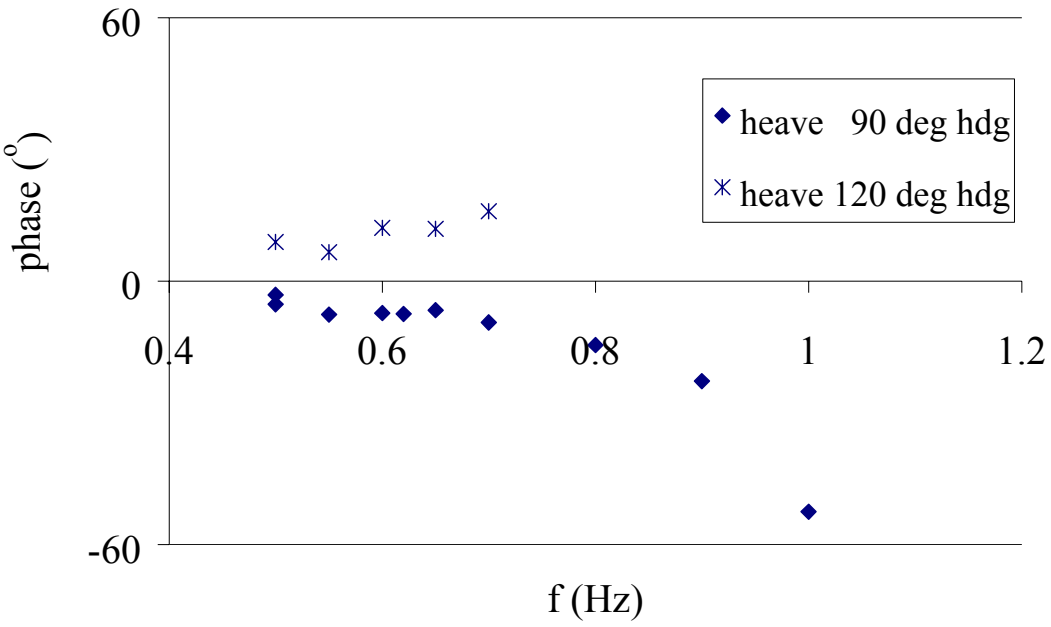

Figure 6-16. heave phase - full keel

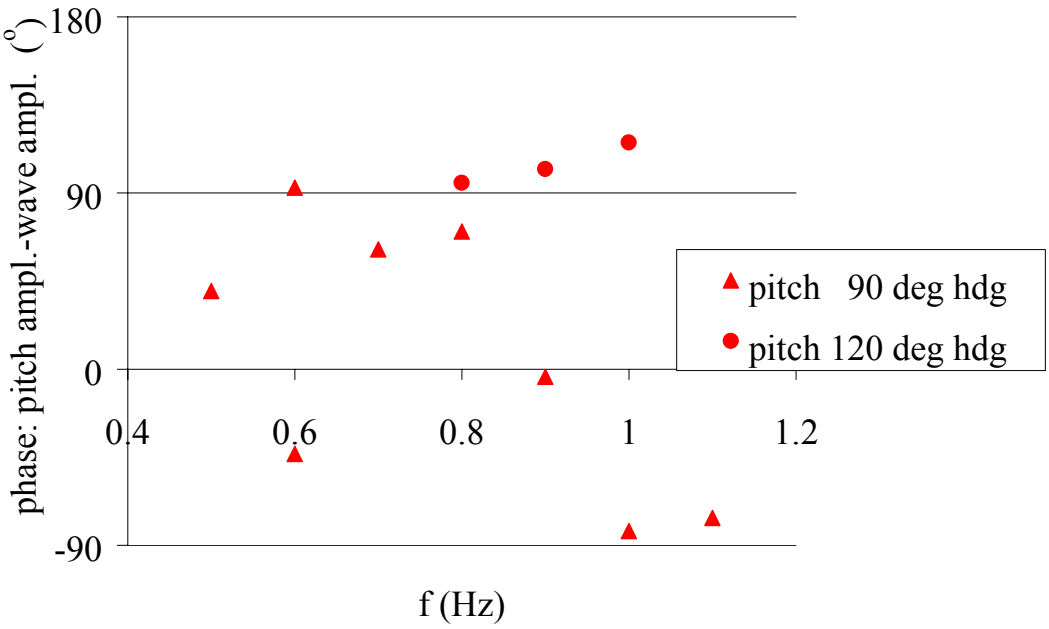

Figure 6-17. pitch phase - full keel

7 CONCLUSIONS AND RECOMMENDATIONS

The inclining experiment and roll table measurement yielded VCG positions in good agreement. The roll table measurement of mass moment of inertia was incorrect. This should be investigated by a sensitivity study of bearing friction and model alignment.

The free roll decay experiments should prove useful for comparison with numerical simulation of unforced roll motion and provided validation data for similar experiments. It is recommended that such experiments be conducted in the CMST acoustics tank.

The wave field exhibited spatial and temporal variations, which required consideration during the processing of the motions measurements. It is recommended that both longitudinal and transverse wave cuts be taken in regular waves over a range of frequencies and amplitudes, prior to further experiments of this sort being conducted at the facility. The influence of the rig attachment system on the wave field should be similarly investigated. The above notwithstanding, the data processing procedure used reduced the influence of temporal wave variation to acceptable levels. There was insufficient information to draw a similar conclusion regarding spatial variation effects.

The roll motion was non-linear with respect to wave amplitude.

The aerofoil keel exhibited slightly less damping than the flat plate keel, with a similar peak response frequency. The half depth keel exhibited a 50% higher peak response frequency than the full depth keel. This difference made comparison of damping effect between the two keels ambiguous. It is recommended that the cause of the difference be investigated, first by numerical estimates of the added inertia, secondly by numerical or experimental estimates of bottom effects on the appendage flow.

The influence of wave heading predicted by numerical methods is supported. The absence of this influence in full scale trials should be investigated further.

End effects on the model should be investigated. This could be initiated by deploying the model with and without the hemispherical ends.

8 REFERENCES

Bhattacharyya, R. 1978, *Dynamics of marine vehicles*, John Wiley and sons, New York.

Klaka, K. 2000, *Response of a vessel to waves at zero ship speed: preliminary full scale experiments*, Centre for Marine Science & Technology, Curtin University, Perth, 2000-21.

Lewis, E. V. 1989, *Principles of Naval Architecture*, Society of Naval Architects and Marine Engineers, Jersey City.

O'Dea, J., Powers, E. & Zselecsky, J. 1992, 'Experimental determination of nonlinearities in vertical plane ship motions', in *19th Symposium on Naval Hydrodynamics*, National Academy Press, USA, Seoul, Korea, pp. 73-92.

Pond, S. & Pickard, G. L. 1983, *Introductory dynamical oceanography,* 2nd edn, Pergamon Press, Oxford.

Robinson, R. W. & Stoddart, A. W. 1987, 'An engineering assessment of the role on non-linearities in transportation barge roll response', *The Naval Architect* no. July/August, pp. 65-79.

Spouge, J. R. 1991, 'Non-linear roll damping measurements', *Transactions Royal Institution of Naval Architects,* vol. 133, no. B, pp. 319-332.

Appendix A: Experimental Log

Table 8-1. Run log - wave runs - no model

run no.	date/time	wave freq (Hz)	wave ampl (m)	calibration file	wave maker file	comment
1	1922 18/06/01	1.0	0.2	dacal1	kk2	waves *10 too big!
2	2005	1.0	0.02	dacal1	kk3	
						increase Tsample to 30sec
3	1014 20/06/01	1.0	0.02	dacal2	kk3	repeat r2
4	1633	1.0	0.02	dacal3	kk3	added 6th probe

Table 8-2. Run log - full keel, 90 degrees wave heading

run no.	date/time	wave freq (Hz)	wave ampl (m)	calibration file	wave maker file	comment
5	1535 20/06/01	1	0.02	dacal4		
6	1555	0.9	0.02	dacal4		
7	1617	0.8	0.02	dacal4	kk5	
8	1640	0.7	0.02	dacal4	kk6	
9	1701	0.6	0.02	dacal4	kk7	
10	1720	0.5	0.02	dacal4	kk8	1st photo in waves
11	1800	0.65	0.02	dacal4	kk9	
	1830					recalibrate ch1; it was jumpy in R9,10
12	1852	0.5	0.02	dcal5	kk8	repeat of R10
13	1912	0.55	0.02	dcal5	kk10	
14	1933	0.62	0.02	dcal5	kk11	
15	1955	0.8	0.01	dcal5	kk12	ripples
16	2015	0.7	0.01	dcal5	kk13	ripples
	0818 21/06/01					water temp 15 deg C
	0930					recalibrated
17	0955	0	0	dcal6		free decay test
18	0958	0	0	dcal6		free decay test
19	1020	0.5	0.01	dcal6	kk14	
20	1040	0.55	0.01	dcal6	kk15	good waves are first ones
21	1102	0.6	0.01	dcal6	kk16	
22	1120	0.65	0.01	dcal6	kk17	
23	1137	0.5	0.03	dcal6	kk18	
24	1200	0.55	0.03	dcal6	kk19	
25	1310	0.65	0.03	dcal6	kk20	2nd video (after wavemaker views)
26	1328	0.6	0.03	dcal6	kk21	

Table 8-3. Run log - foil keel, 90 degree wave heading

run no.	date/time	wave freq (Hz)	wave ampl (m)	calibration file	wave maker file	comment
27	1500 21/06/01	0.6	0.02	dcal6	kk7	c/f r9
28	1520	0.5	0.02	dcal6	kk8	c/f r10

run no.	date/time	wave freq (Hz)	wave ampl (m)	calibration file	wave maker file	comment
29	1537	0.65	0.02	dcal6	kk9	c/f r11
30	1554	0.7	0.02	dcal6	kk6	c/f r8
31	1610	0.55	0.02	dcal6	kk10	c/f r13
32	1630	0.65	0.02	dcal6	kk9	rpt r29

Table 8-4. Run log - half keel, 90 degree wave heading

run no.	date/time	wave freq (Hz)	wave ampl (m)	calibration file	wave maker file	comment
33	1800 21/06/01	0.5	0.02	dcal6	kk8	c/f r10
34	1830	0.6	0.02	dcal6	kk7	c/f r9. Pt LVDT slack at highest amplitude
35	1920	0.6	0.02	dcal6	kk7	rpt r34. aft post noisy in bearing (sloppy)
36	1950	0.7	0.02	dcal6	kk6	c/f r8
37	2007	0.8	0.02	dcal6	kk5	c/f r7
38	2028	1.0	0.02	dcal6	kk22	c/f r5
39	2045	0.9	0.02	dcal6	kk23	corrupted floppy :data lost
40	2105	0.9	0.02	dcal6	kk23	
41	2118	1.1	0.02	dcal6	kk24	
						take photos 22 (plan) and photo 23 (basin from ladder)

Table 8-5. Run log - full keel, 120 degree wave heading

run no.	date/time	wave freq (Hz)	wave ampl (m)	calibration file	wave maker file	comment
	1030?			dcal7		recalibrated LVDTs
999	1100 22/06/01			dcal7		static noise run
42	1130	0	0	dcal7	kk7	inclined upright
43	1135	0	0	dcal7	kk8	inclined stbd
44	1140	0	0	dcal7	kk9	inclined upright
				dcal8		recalibrated wave probe
45	1210	0.5	0.02	dcal8	kk8	c/f r10
46	1305	0.6	0.02	dcal8	kk7	c/f r9
47						there is no run 47!
48	1327	0.7	0.02	dcal8	kk6	c/f r8. photo taken
49	1345	0.65	0.02	dcal8	kk9	c/f r11
50	1405	0.55	0.02	dcal8	kk10	rpt r13.

Table 8-6. Run log - half keel, 120 degree wave heading

run no.	date/time	wave freq (Hz)	wave ampl (m)	calibration file	wave maker file	comment
51	1525	0.8	0.02	dcal8	kk5	c/f r7
52	1543	0.9	0.02	dcal8	kk23	
53	1605	1.0	0.02	dcal8	kk22	